

CFD PRE-TEST ANALYSIS OF THE FUEL PIN BUNDLE SIMULATOR EXPERIMENT IN THE NACIE-UP HLM FACILITY

I. Di Piazza

ENEA
Camugnano, 40032, Brasimone, Italy
ivan.dipiazza@enea.it

R. Marinari

UNIFI
UNIFI DICI, Largo Lucio Lazzarino 2 – 56122 Pisa, Italy
ranieri.marinari@gmail.com

M. Angelucci

UNIFI
UNIFI DICI, Largo Lucio Lazzarino 2 – 56122 Pisa, Italy
morena.angelucci@gmail.com

ABSTRACT

In the context of the studies on GEN. IV/ADS nuclear systems, the correct evaluations of the temperature distribution in the fuel pin bundle is of central interest. In particular, the use of lead or lead-bismuth eutectic (LBE) as coolant for the new generation fast reactors is one of the most promising choices. At ENEA-Brasimone R.C., large experimental facilities exist to study HLM free, forced and mixed convection in loops and pools: e.g. NACIE-UP is a large scale LBE loop for mixed convection experiments. In the context of the SEARCH FP7 project, an experiment has to be performed in the NACIE-UP facility to assess the coolability of a 19-pin wire-wrapped electrical bundle (Fuel Pin Simulator, FPS), with heat flux up to 1 MW/m². The bundle is representative of the one adopted in the MYRRHA concept.

A CFD analysis of fluid flow and heat transfer was carried out in the heavy liquid metal (LBE) cooled bundle test section of the NACIE-UP facility. The model includes the details of the wire-spacers as well as the entry region of the test section. A turbulence closure approach is adopted for all the simulations with $\approx 3.5 \cdot 10^7$ nodes and a resolution of $y^+ = 1 - 4$ at the wall in the range of interest.

Results are compared with the up-to-date correlations on pressure loss and heat transfer and the experimental range is completely explored by CFD. The thermal structures of the test section are modelled and the role of conjugate heat transfer was assessed.

Several highlights emerged from the numerical study for the experimental campaign. In particular, the accuracy in the measurement of heat transfer between rods and fluid was evidenced as weak point of the experimental test matrix. As a consequence the test matrix was modified.

KEYWORDS

Liquid Metal, Fast Reactor, Thermal-hydraulics

1. INTRODUCTION

In the context of the studies on GEN. IV/ADS nuclear systems, the correct evaluations of the convective heat transfer in the core is of central interest. In particular, the use of Lead or Lead-Bismuth Eutectic (LBE) as coolant for the new generation fast reactors is one of the most promising choices.

Due to the high density and high conductivity of Lead or LBE, a detailed analysis of the thermo-fluid dynamic behavior of the Heavy Liquid Metal (HLM) inside the sub-channels of a fuel rod bundle is necessary in order to support the Front-End Engineering Design (FEED) of gen. IV/ADS fast spectrum demonstrative facilities like MYRRHA [1] (Multi-purpose hybrid research reactor for high-tech applications). In this frame, the synergy between numerical analysis by CFD and data coming from large experimental facilities seems to be crucial to assess the feasibility of the components. At the ENEA-Brasimone Research Centre, large experimental facilities exist to study HLM free, forced mixed convection in loops and pools: i.e. CIRCE [1] is currently the largest experimental HLM pool facility in Europe and NACIE-UP is a large scale LBE loop for mixed convection [3].

The NACIE-UP experiment was designed in order to describe the thermal-hydraulic behavior of the MYRRHA FA during a Loss of Flow Accident (LOFA) with the coast-down of the main circulation pump. The accident is protected loss of flow (PLOFA) if control rods can be inserted and the neutronic multiplication stops. In that case only the decay heat must be evacuated depending on the burn-up level, and at maximum 7% of the power should be considered in this case. Instead, the accident is unprotected (ULOFA) if the control rods cannot be inserted and the full power must be evacuated.

Heat transfer during a LOFA is driven by the inertia of the fluid during the pump coast-down and the onset of natural circulation due to the difference in height between the heat source and the heat sink. As a consequence of a LOFA, a stationary natural circulation flow rate will be established in a characteristic time which depends on the specific geometry of the system under consideration and on the geometry of the bundle.

To simulate the fuel pins, an electrically heated rod bundle was specifically designed and provided for this purpose.

The main difference between the MYRRHA bundle and the NACIE-UP bundle is the number of ranks and pins: 7 ranks and 127 pins for MYRRHA against 3 ranks and 19 pins for NACIE-UP. This difference in the number of pins is not relevant for the convective heat transfer in the sub-channels because side, corner and central sub-channels can be monitored in the 19 pin bundle and basic phenomenology is the same as in the MYRRHA bundle. For a fixed average velocity in the bundle, pressure drops are expected to be a little higher in the NACIE-UP bundle because the influence of the wall is stronger, but from the literature and from numerical evidences, it is clear that this difference is not really relevant [4].

A computational study was carried out on the experimental wire-wrapped bundle test section of NACIE-UP. The CFD model includes liquid metal and solid structures and it reproduces the real geometry of the section including the inlet and outlet regions. Wire-wrapped bundles are widely investigated in the literature due to their dominant application in the sodium technology. Therefore, lot of works are present from the '60's to '80s when the interest for sodium technology was high [5-8]. In the last years, the interest in the liquid metal technology is high again due to the GEN. IV commitment and objectives: non-proliferation, economics, reduction of the long-life waste, safety, and higher efficient use of the fuel. With powerful modern computers, several numerical CFD studies appeared on the wire-wrapped bundles. For example, the Indian research is currently focused on the development of PFBR and LMFBR and try to develop numerical methodologies to analyze wire-wrapped configurations [9-10]. Numerical studies on wire-wrapped pin bundle cooled by heavy liquid metal are difficult to find in the literature.

2. THE NACIE-UP EXPERIMENTAL LOOP

2.1 General framework

The reference for the piping and instrumentation is the P&ID reported in Figure 1, where all the instrumentation, components and pipes are listed and logically represented. The facility includes:

- The Primary side, filled with LBE, with 2 ½" SS AISI304 pipes, where the main new components and instruments will be placed:
- A new Fuel Pin Simulator (19-pins) 250 kW maximum power;
- A new Shell and tube HX with two sections, operating at low power (5-50 kW) and high power (50-250 kW);
- A new low mass flow rate induction flow meter (0-3 kg/s) FM101;
- A new high mass flow rate induction flow meter (3-15 kg/s) FM102;
- 5 bubble tubes to measure the pressure drops across the main components and the pipes;
- Several bulk thermocouples to monitor the temperature along the flow path in the loop;
- The Secondary side, filled with water at 16 bar, connected to the HX, shell side. It includes a pump, an air-cooler, by-pass and isolation valves, and a pressurizer (S201) with cover gas;
- An ancillary gas system, to ensure a proper cover gas in the expansion tank and to provide gas-lift enhanced circulation;
- A LBE draining section, with ½" pipes, isolation valves and a storage tank (S300);
- A gas-lift circulation system in the riser ensures about 0.6 bar of driving force.

The LBE melting temperature is about 130 °C; therefore, the typical operating temperatures in the loop are above 200 °C. The difference in height between the heating section and the Heat exchanger is about 5 m to perform natural circulation tests. Due to the high LBE density ($\approx 10300 \text{ kg/m}^3$), the hydrostatic pressure gradient in the facility is around 1 bar/m.

2.2 The experimental bundle test section

The FPS will consist of 19 electrical pins with an active length $L_{\text{active}} = 600 \text{ mm}$. The whole length ($L_{\text{total}} = 2000 \text{ mm}$) includes the non-active length and the electrical connectors. The pin has a diameter $D = 6.55 \text{ mm}$, and the maximum wall heat flux will be close to 1 MW/m^2 . The pins are placed on a hexagonal lattice by a suitable wrapper, while spacer grids will be avoided thanks to the wire spacer. The total power of the fuel pin bundle is $\sim 235 \text{ kW}$.

This fuel pin bundle configuration is relevant for the MYRRHA's core thermal-hydraulic design [1].

The goals of the experimental campaigns planned on the NACIE-UP facility with the new bundle are: the measurement of the pin cladding temperature by embedded thermocouples; the measurement of the sub-channels temperature; Heat Transfer Coefficient (HTC) evaluation; the check of hot spots and peak temperatures; the evaluation of the axial thermal stratification entrance length along the sub-channels.

A schematic representation of the cross-section of the pin bundle is shown in Figure 2. The total flow area can be conventionally divided into 54 sub-channels of different ranks (S1-S54). The sub-channels and the relative pins that will be instrumented are also indicated in Figure 2. Wires are helicoidally twisted around each pin.

The main geometrical dimensions to be considered for a thermal-hydraulic assessment of the FA are:

- The rod diameter $D=6.55 \text{ mm}$;
- The wire diameter $d=1.75 \text{ mm}$;
- The pitch to diameter ratio $P/D=1.2824$;
- The streamwise wire pitch $P_w=262 \text{ mm}$;
- The regular lattice is triangular/hexagonal staggered;
- The resulting flat to flat distance of the hexagonal wrap is 39.34 mm ;
- The equivalent hydraulic diameter of the bundle is $D_{\text{eq}}=4.147 \text{ mm}$;
- The equivalent diameter sub-channel is $D_{\text{SC,eq}} = 3.84 \text{ mm}$;

The three pin ranks of the bundle are representative of all the sub-channels in the MYRRHA FA. In fact, it is well known from the literature that for wire-wrapped bundles of similar geometry, the influence of the wall is considered important for the external rank N and for the $N-1$ rank of pins, while the other ranks are not so much influenced by the wrap wall. For each sub-channel, the bulk and wall temperatures will be monitored in three different cross sections in the active region. The total number of bulk thermocouples ($\phi=0.5 \text{ mm}$) is 15, while the total number of wall embedded thermocouples ($\phi=0.35 \text{ mm}$)

is 52. The fuel pin bundle simulator (FPS) consists of the hexagonal wrap and additional parts and flanges to connect the bundle to the NACIE-UP facility. A picture of the FPS is shown in Figure 3. A developing non-heated wire-wrapped region of 2.5 wire pitch is present in order to allow the flow to be fully developed at the beginning of the active region.

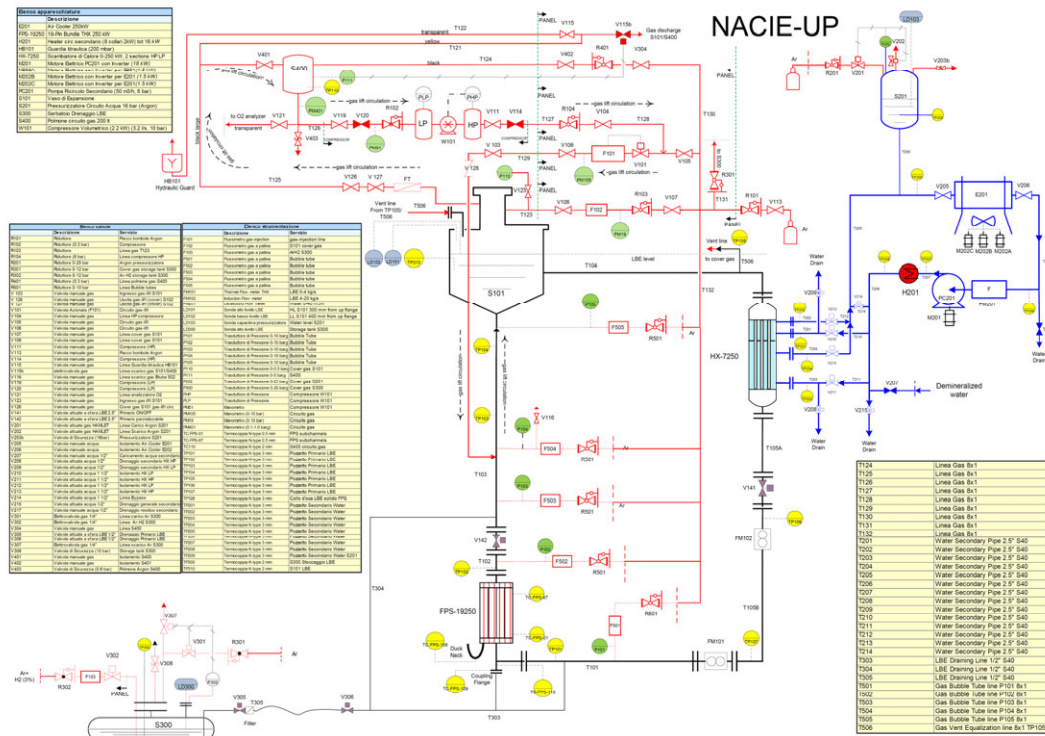


Figure 1 Piping and Instrumentation Diagram (P&ID) of the NACIE-UP facility.

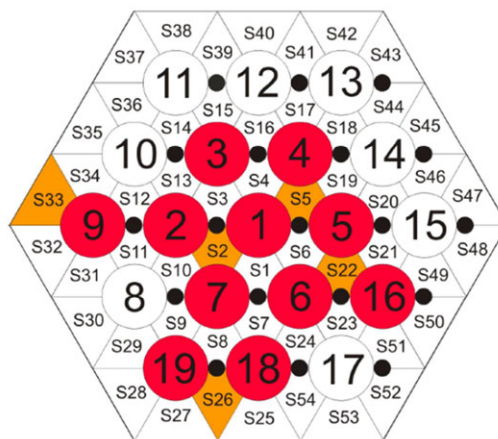


Figure 2 Cross-section of the pin bundle simulator for the NACIE-UP facility. Instrumented pins in red; instrumented sub-channels in orange, wire in black.

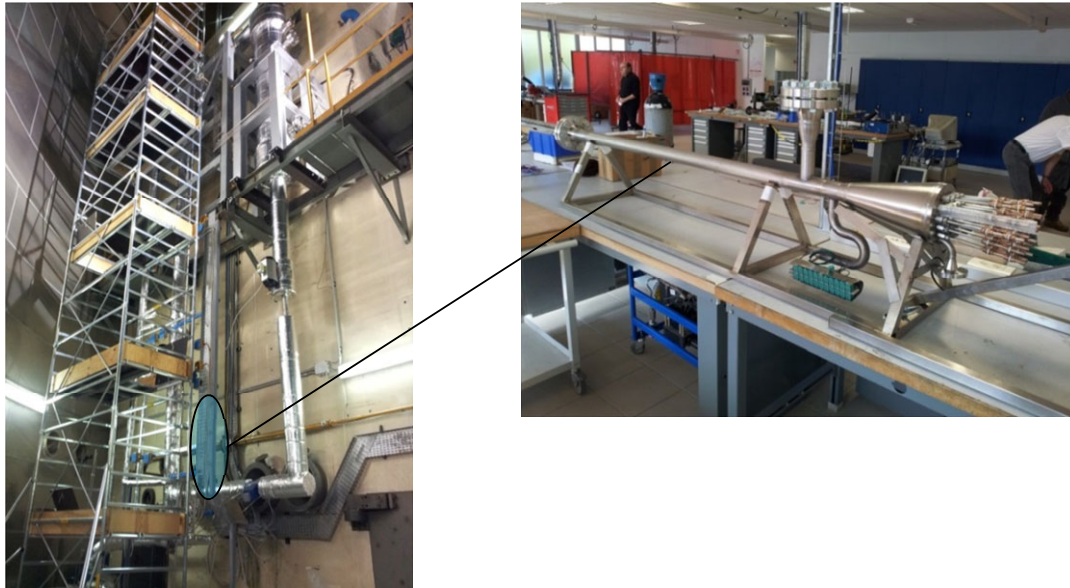


Figure 3 The NACIE-UP facility with an highlight of the FPS and its location

3. THE CFD MODEL OF THE FPS BUNDLE

A CFD analysis was performed on the pin bundle test section as pre-test of the experimental campaign. A technical drawing of the test section is reported in Figure 4.

The whole FPS test section was modelled including the inlet region, the entry region, the active region, the outlet region with the upper grid, and the hexagonal wrap, see Figure 5. The exact geometry of the pins with wire was also reproduced by collapsing the wire into the pin clad by a small surface contact, see detailed mesh view in Figure 5. This practice allows better mesh generation on the fluid side and it is commonly used in the literature, see for example [9].

The model shown in Figure 5 includes the conjugate heat transfer in the pin clad, in the wire and into the hexagonal wrap. It should be stressed that the hexagonal wrap in the experimental test section is obtained from a stainless steel full rod by electrochemical erosion; this implies that the wrap is very thick and the conjugate heat transfer effects may be relevant.

Regarding the mesh generation strategy, the inflation was used close to solid-fluid interfaces on the fluid side (structured hexahedral elements). This choice guarantees good mesh properties close to the wall and it implies a better numerical discretization for the wall phenomena. In the bulk of the fluid, the unstructured mesh was adopted. In the solid domains, an hexahedral dominant mesh was used. The total number of nodes and elements in the model are $3.5 \cdot 10^7$ and $9.7 \cdot 10^7$ respectively.

The simulations are stationary RANS and they were performed by using ANSYS-CFX 15 [13] with the Shear Stress Transport (SST) $k-\omega$ turbulence model [11] and a second-order (CFX 'High Resolution') scheme for convective terms. The turbulent Prandtl number has been set to 1.5, as suggested by several studies on heat transfer in heavy liquid metals at moderate Peclet numbers [12]. Moreover, in a more extensive study [15], it is shown that the influence of the turbulent Prandtl number is negligible in the laminar range and moderate for the higher mass flow rates investigated here. The full convergence at 10^{-5} residuals maximum was achieved for all cases.

A total mass flow rate ($\dot{m} = 0.5 - 7 \text{ kg} / \text{s}$), constant temperature ($T_{inlet} = 200 \text{ }^\circ\text{C}$), boundary conditions were imposed at the inlet coherently with the test matrix of the experimental campaign, while pressure

boundary conditions were imposed at the outlet. At the internal pin wall in the active region, a constant heat flux q'' was imposed. The computational mesh adopts a resolution close to the wall such to achieve a y^+ of the order of 1 for 2 kg/s and of the order of 4 for 7 kg/s. These features guarantee high accuracy to the model, minimize the discretization error and allow to integrate turbulence model equations down to the viscous sublayer.

Constant thermo-physical properties were assumed for LBE at 250°C, according to Table 3-1 [13]. For the clad, wrap and wire material (SS AISI 304), constant physical properties were considered at 250 °C (Table 3-2).

ρ [kg/m^3]	Density	10403
ν [m^2/s]	Kinematic viscosity	$2.007 \cdot 10^{-7}$
k [W/mK]	Thermal conductivity	11.34
c_p [J/kgK]	Specific heat at constant pressure	146.7
Pr	Prandtl number	0.0259

Table 3-1 Physical properties of LBE at 250 °C.

ρ [kg/m^3]	Density	7854
k [W/mK]	Thermal conductivity	16.2
c_p [J/kgK]	Specific heat at constant pressure	434

Table 3-2 SS AISI 304 properties

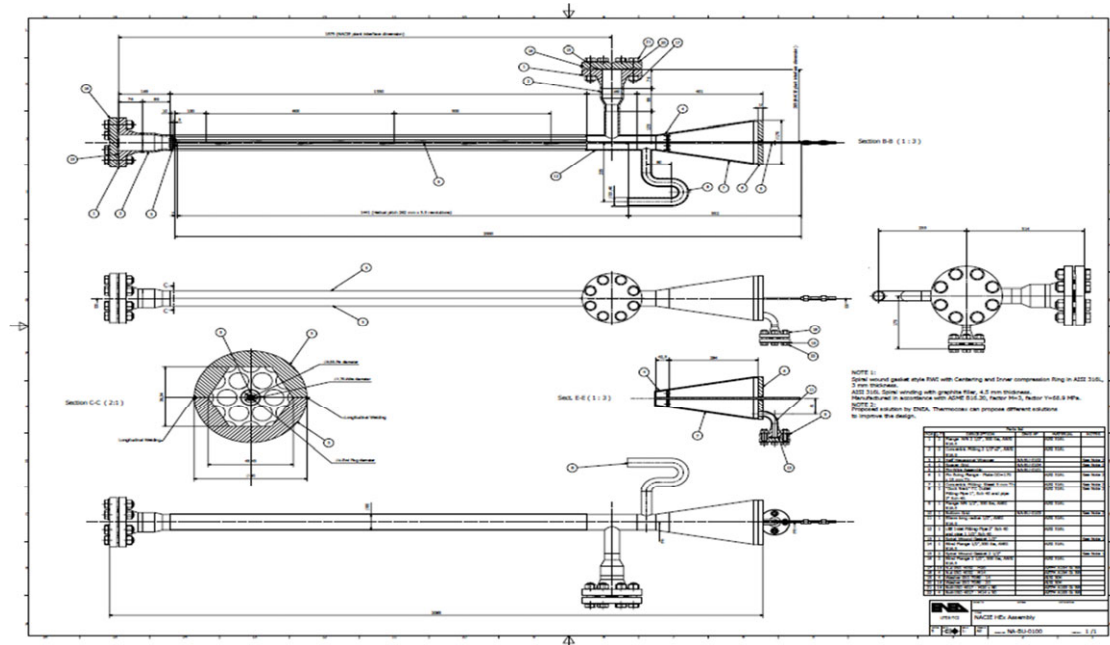


Figure 4 Overall bundle layout: technical drawing

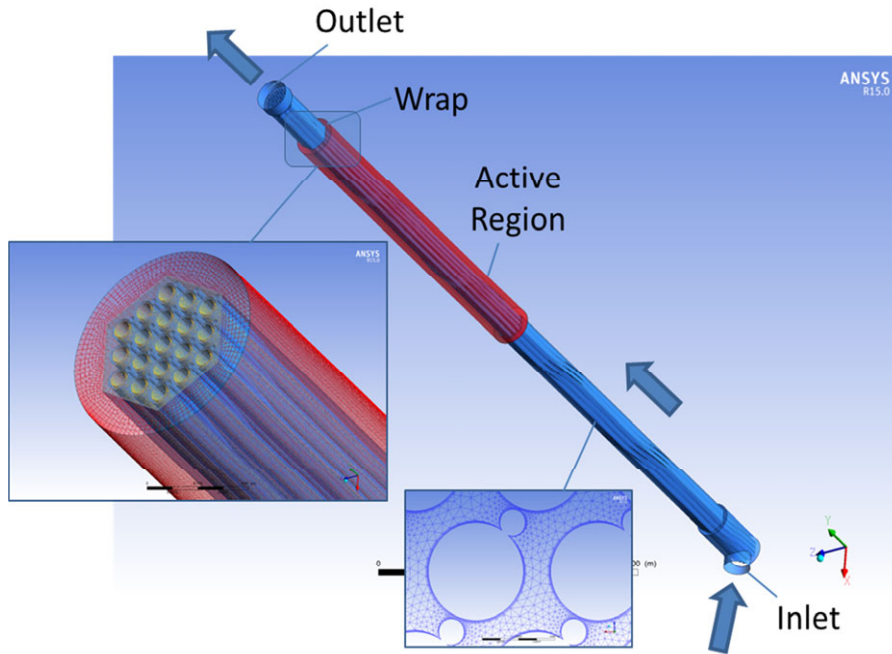


Figure 5 NACIE-UP CFD model layout with details of computational mesh

4. SENSITIVITY STUDIES

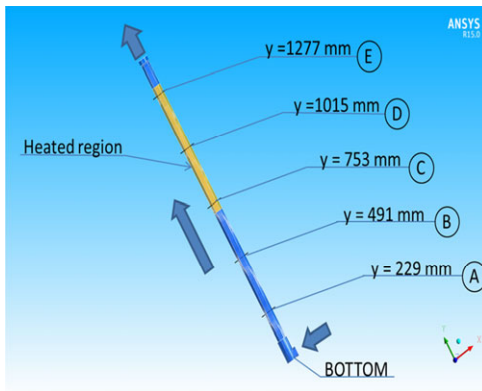


Figure 6 Detailed representation of the cross-section planes with their nomenclature and their height from the BOTTOM plane.

Different sensitivity analyses were carried out to fix the CFD model of the NACIE-UP pin bundle.

For a correct sensitivity analysis and a detailed analysis of the CFD results, different cross-section planes were adopted, one wire pitch (262 mm) far one from the other. In Figure 6 the position of the planes is reported by indicating the distance from the BOTTOM plane and the nomenclature adopted in the next paragraphs. It has to be pointed out that there are three cross-section planes into the heated region (in orange), at the same heights of the FPS thermocouples, i.e. actually coincident with the measuring planes.

All the sensitivity analyses reported here (except where specifically described) adopted a specific reference case with an inlet mass flow rate of 2.032 kg/s, a sub-channel Reynolds number of 6162 and a total thermal power of 32.52 kW uniformly distributed in the heated length; the

same data are reported in Table 4-1. The case is in the transitional region and at the center of the NACIE-UP experimental test matrix.

Table 4-1 Data setting of the reference case studied in the sensitivity analysis.

\dot{m}_{NACIE} [kg/s]	u_{sc} [m/s]	Re_{sc} [-]	Thermal power [kW]
2.032	0.29	6162	32.52

4.1 The influence of mesh size

Three different meshes were developed on the fluid domain:

- ✓ a coarse mesh 'C' with 10 million total nodes;
- ✓ a medium mesh 'M' with ~ 22 million nodes;
- ✓ a fine mesh 'F' with ~ 29 million nodes.

All the meshes have a resolution of $y^+ \sim 1$ at the wall with inflation for the reference case.

Comparison was performed on the reference case on the following fields: secondary velocity, temperature.

An interesting comparison takes into account the swirl (secondary) velocity field on the same cross-section (Figure 7). The swirl velocity is here defined as the magnitude of the component of the velocity

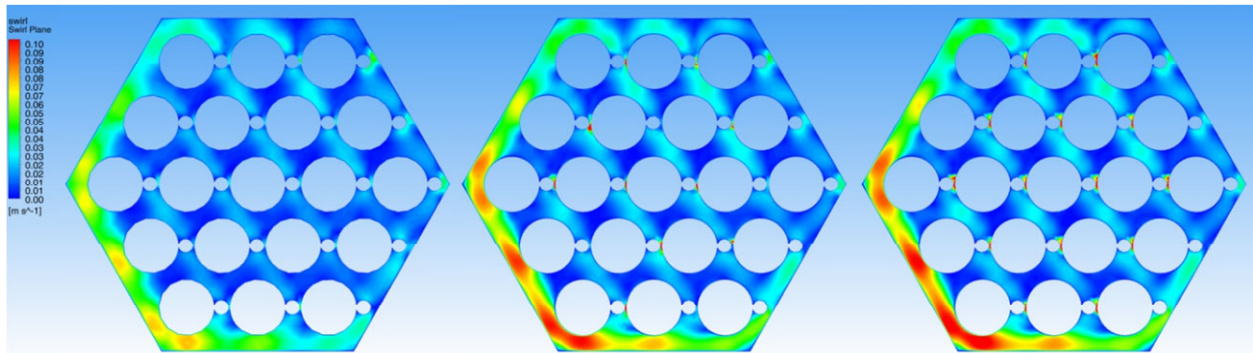


Figure 7 Swirl velocity profiles at the middle of the active zone for : coarse size mesh (left), medium size mesh (center) and fine size mesh (right).

vector orthogonal to the mainstream direction, i.e. in the plane of the cross-section. From the comparison, it is possible to notice again that the coarse size mesh C under-predicts the magnitude of the swirl velocity component even if it's able to predict the maxima locations. The medium (M) and fine size (F) meshes, on the other hand, give practically the same results.

Looking at the thermal field, the temperature contours on the same plane of the previous comparisons are

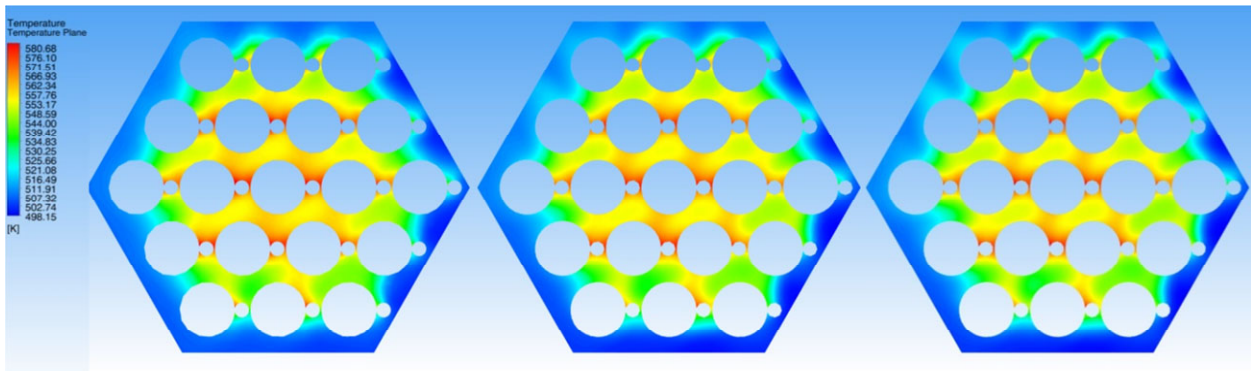


Figure 8 Temperature profiles at the middle of the active zone for : coarse size mesh (left), medium size mesh (center) and fine size mesh (right).

extrapolated for the three cases and reported in Figure 8. The same conclusions of the previous cases could be depicted, with a substantial grid independence of the quantity.

As a conclusion of the mesh independence study, the medium size mesh was chosen for the subsequent sensitivity studies and test-matrix simulations.

4.2 The influence of solid structures

The inclusion of the solid structures into the CFD model was developed for taking into account the conjugate heat transfer effect of the outward hexagonal wrap. In particular the hexagonal wrap has a considerable thickness due to the specific mechanical construction derived from a full SS pipe by a milling cutter. Therefore low resistance solid region thermal ‘bridges’ exist between hot and cold outwards regions of the LBE. Pins and wires were also modelled and meshed with at least one node into the pin clad, for a more realistic simulation of the heat transfer phenomena between the solid pins and the fluid LBE.

Figure 9 shows the temperature contours in section D for the model without solid structure (left) and with solid structures (right). The conjugate heat transfer effect of the outward hexagonal pipe causes a more uniform temperature distribution in the external sub-channels of the pin bundle, smoothing the cold regions in the lower-right part of the cross-section.

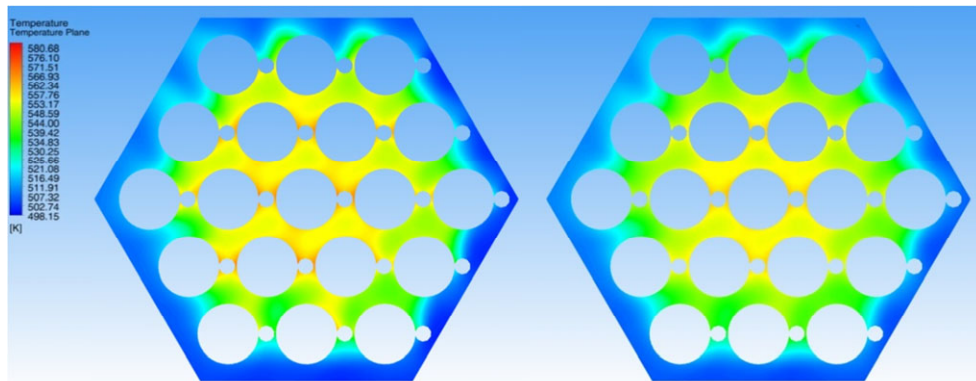


Figure 9 Comparison of temperature contours on the same cross-section for the preliminary

Local temperature differences in the same points between the two models can be 10-15 °C or more. All these phenomena cannot be neglected and allow to assess that for a reliable simulation of the NACIE-UP pin bundle thermal field, the outward pipe structures must be included into the CFD model to describe the conjugate heat transfer.

From the same comparison, the pins’ modelling effect on the thermal field can be deduced; the residual hot-spots in the small gaps between the wire spacers and the pins adjacent to it tend to disappear thanks to the smoothing effect of the heat transfer between the pin and the wire and through the wire from one side of the fluid to another.

5. PRE-TEST ANALYSIS

The method adopted was validated against ORNL experimental data [14] in a separate work [15], and it is not reported here.

For the pre-test analysis of the NACIE-UP pin bundle, a specifically numerical test matrix was developed with mass flow rates ranging from 0.5 kg/s to 7 kg/s, according to the gas lift system capabilities and the experimental test matrix, and heating power inputs imposed for having an inlet-outlet temperature difference of 110 °C (as in the experimental test matrix). The numerical test matrix is doubled because the same cases are simulated either with the preliminary model (only fluid -OF-) and with the complete model (with solid structures -SS- included) . The test matrix is reported in Table 5-1.

Table 5-1 Numerical test matrix developed for the pre-test analysis of the NACIE-UP pin bundle; the average sub-channel velocity u_{sc} , the Reynolds number and the Peclet number are also reported.

Preliminary model cases	Complete model cases	\dot{m}_{NACIE} [kg/s]	Power [kW]	\bar{u}_{sc} [m/s]	Re_{sc}	Pe_{sc}
OF05	SS05	0.5	8.07	0.07	1516	41.0
OF10	SS10	1.0	16.14	0.15	3032	82.0
OF20	SS20	2.032	32.52	0.29	6162	166.5
OF30	SS30	3.0	48.42	0.44	9097	245.8
OF40	SS40	4.0	64.56	0.58	12130	327.7
OF50	SS50	5.0	80.70	0.73	15162	409.6
OF60	SS60	6.0	96.84	0.88	18195	491.5
OF70	SS70	7.0	112.97	1.03	21227	573.5

For sake of simplicity, only the analysis of the transitional flow regime case (SS20 and OF20) will be described because the other cases studied show similar behaviors.

Figure 10 reports the development of the axial velocity component on the five cross-section planes, all the contours have the same scale reported in the upper left corner for completeness; the axial component is already developed well before the heated region, and it's fully developed after two wire pitch lengths. Figure 11 shows the vector plots of the swirl velocity component in the cross-section planes. The swirl velocity could reach the 30 % of the average velocity in the cross-section u_{sc} (Table 5-1), and it is highly asymmetric: negligible in the inner sub-channels and strong in the corner and edge sub-channels with a magnitude strongly influenced by the wire position.

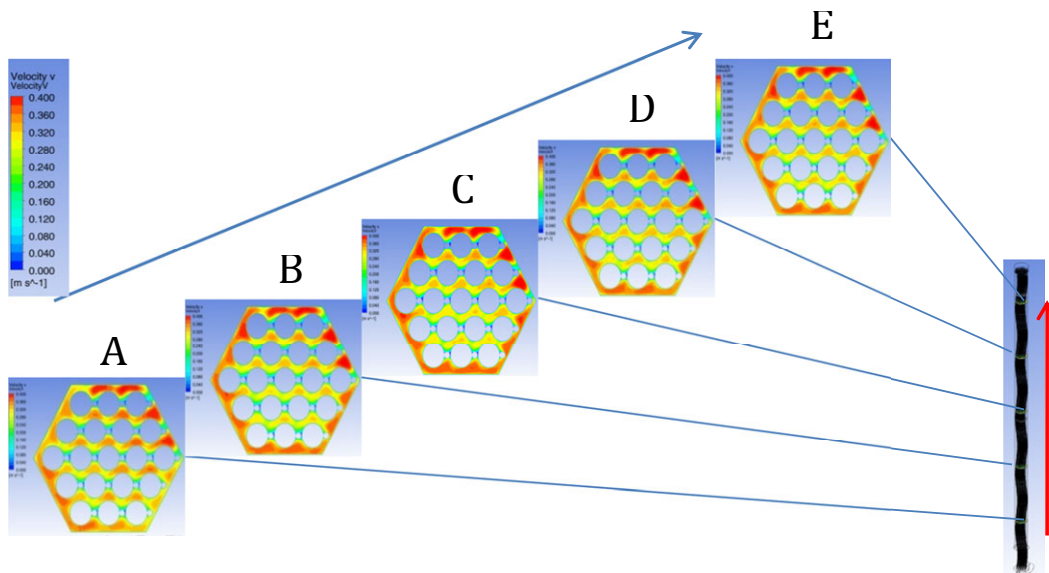


Figure 10 Development of the mainstream velocity component for the 2.032 kg/s case.

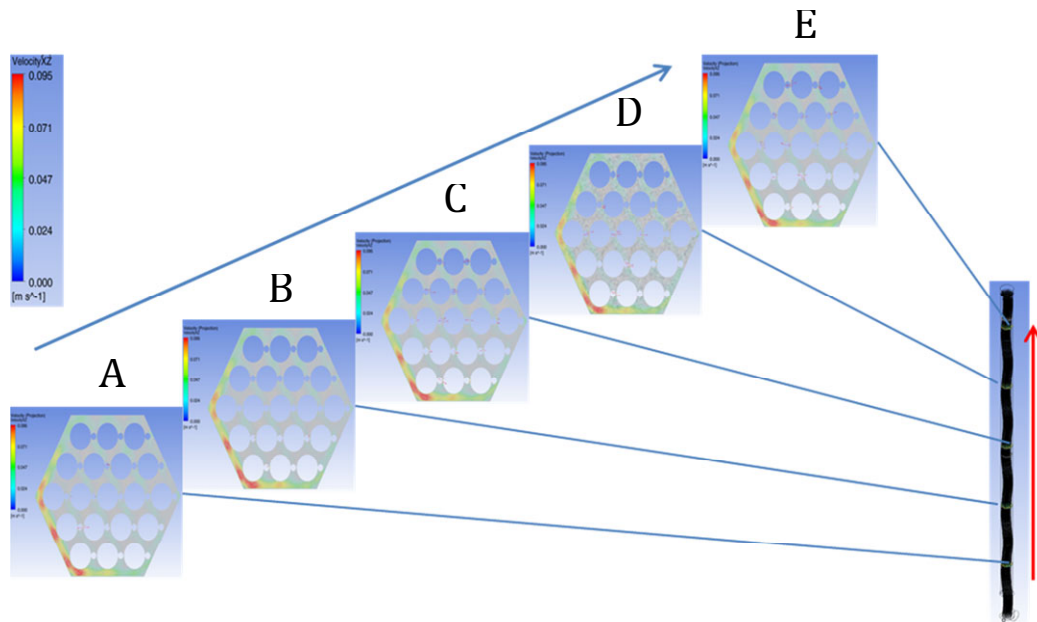


Figure 11 Development of the swirl velocity component for the 2.032 kg/s case.

Looking at the temperature contours ($T_{\text{abs}} = T - T_{\text{bulk}}$) on the three different planes of the heated region (Figure 12), it was found that the temperature field is not fully developed.

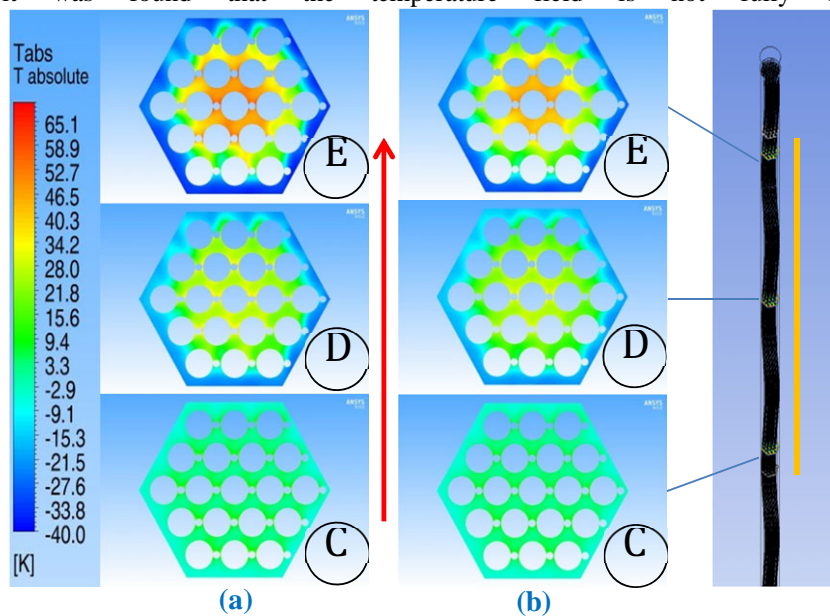


Figure 12 Contours of the Tabs on planes C, D and E in the heated zone (in orange) for the OF20 case (a) and SS20 case (b).

5.1 Overall pressure drop

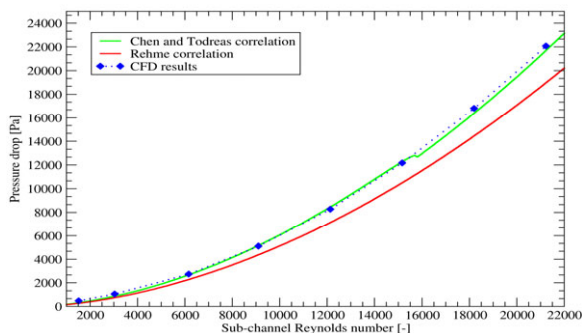


Figure 13 Comparison between the CFD results and the available correlations for the pressure drop in the

The results compared are the pressure drop predictions in the active region of the bundle for the different mass flow rates (i.e. different Reynolds numbers).

Figure 13 shows the pressure drop against the sub-channel Reynolds number from CFD results and from the correlations. CFD results are really in good agreement with the Chen and Todreas correlation, while Rehme's predictions underestimate the pressure drop. The behavior of the two correlations with respect to the numerical results is perfectly in accordance with the literature with a systematic under-estimation of the Rehme correlation in the whole range.

5.2 The heat transfer issue

During the detailed investigation of the test matrix, it was pointed out that the thermal field is not fully developed in any case investigated. This fact precludes any comparison of our results with the available heat transfer correlations from the literature.

Looking for a better study of the heat transfer phenomena involved into the pin bundle, a new CFD model was developed for studying the heated bundle in fully developed conditions of velocity and temperature.

5.3 The wire pitch model

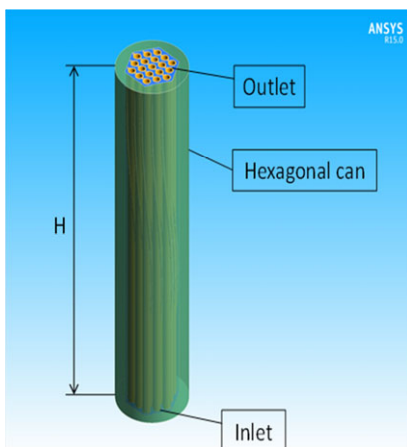


Figure 14 Wire pitch CFD model

The new model developed can be seen as a portion of the complete model; in fact it has the same radial bundle dimensions of the complete model but a total length equal to one wire pitch (262 mm); the solid structures of the 19 pins and wires (in orange) and the hexagonal pipe (in green) are included (Figure 14).

The mesh elements and the mesh size for the solid and fluid bodies are of the same order of the complete model and similar considerations yield.

The heat flux (q'') is imposed on the inner surface of the pins, while the total thermal power is scaled with the model dimensions, the external surface of the hexagonal pipe is imposed adiabatic.

A periodic boundary condition is imposed on the inlet and outlet surfaces of the fluid model for achieving the fully developed conditions of velocity and temperature.

Specific source terms in the Navier-Stokes equations were added in order to achieve a periodic solution. A simple representation of the results is shown graphically in Figure 15, where all the results obtained were compared with the Ushakov [18] and Mikityuk [19] heat transfer correlations .

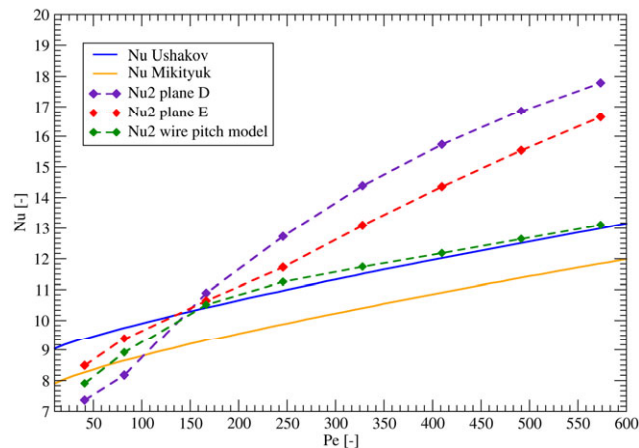


Figure 15 Nu_2 values calculated for the numerical test matrix against the Peclet number compared with the Ushakov correlation and Mikityuk correlation

Figure 15 shows that the thermal field is not fully developed in the complete model: the Nusselt number based on wall and central channel temperature (Nu_2) tends to decrease to the asymptotic trend of the wire pitch model results for mass flow rates higher than 2 kg/s. In the same graph are also reported two best fitting heat transfer correlations (the Ushakov and the Mikityuk ones) : the asymptotic values found are anyway higher than the predictions of the Ushakov correlation but tend to its value at higher mass flow rates. Nevertheless, it must be underlined that there are not correlations specifically developed for wire-wrap bundle geometry with heavy liquid metals, and the two correlations adopted basically refer to grid spaced LM cooled bundles. The wire wrap geometry tends to increase the heat transfer because of the swirl flow and the

increased turbulence level.

The lower mass flow rate cases simulated (SS05 and SS10 cases) show a rather different behavior of the Nusselt number; the values calculated for the complete model simulations, in facts, are higher than the asymptotic ones of the wire pitch model simulations but anyway more similar to the correlation predictions; the asymptotic Nusselt number values of the wire pitch cases are lower than the Ushakov prediction but anyway near the Mikityuk values.

6. CONCLUSIONS

A CFD pre-test analysis was carried out on the NACIE-UP fuel pin bundle simulator (FPS) placed at the ENEA Brasimone Research Centre. The FPS has 19-pins, it is wire-wrapped, it is cooled with liquid Lead Bismuth Eutectic (LBE) and the study is in the context of GEN.-IV nuclear reactors research.

An experimental campaign will be carried out in 2015 on the bundle coolability in the context of the SEARCH FP7 EU project to support the MYRRHA design. The paper reports the CFD model developed to describe the experimental test section, the sensitivity analysis, model validations and pre-test results.

The whole FPS test section was modelled including the inlet region, the entry region, the active region, the outlet region with the upper grid, and the hexagonal wrap. The total number of nodes and elements in the model was $3.5 \cdot 10^7$ and $9.7 \cdot 10^7$ respectively, with wall resolution $y^+ = 1 - 4$ in the range of interest. Stationary RANS computations were performed for the whole experimental range with mass flow rates from 0.5 to 7 kg/s and with a corresponding Reynolds number from $1.5 \cdot 10^3$ to $2.1 \cdot 10^4$.

A CFD code validation was carried out on experimental data by ORNL in a similar geometry cooled by sodium.

The velocity field in the wire-wrapped assembly of NACIE-UP shows complex features and a strong secondary fluid flow due to the swirl. Results show that the hydrodynamic field is well developed well before the beginning of the active region after one wire pitch about. Nevertheless, the thermal field is not fully developed in the active region and the slopes of the wall and bulk temperatures are different. This fact is not new and it was evidenced by other authors [10]. A good agreement was obtained by comparing

CFD results with existing pressure drop correlations on wire-wrapped bundles; in particular a very good agreement was obtained with the Chen & Todreas correlation [17].

Regarding the conjugate heat transfer effect, from numerical simulations it is clear that the conduction in the wrap pipe structure and in the wire is very important to correctly capture the temperature gradients, the local temperature maxima close to the wire and temperature minima in the edge sub-channels, especially for the lower Reynolds number cases. The undeveloped thermal field of the test matrix cases simulated, the absence of heat transfer correlations specifically developed for wire wrap pin bundle geometry and the uncertainty in the nomenclature and definitions precluded a structured validation of the results, developing an asymptotic wire pitch domain and adopting different definitions of HTC and Nu for a comparison with the available heat transfer correlations for liquid metal cooled bundles.

Several highlights for the experimental activity emerged by the pre-test CFD analysis. In particular, the fuel bundle power should be increased as much as possible in the low mass flow rate range to improve the accuracy on the heat transfer coefficient measurement. Moreover, the numerical evidence of the not fully developed thermal field in the bundle, implies that experimental results must be released with details on the experimental test facility and boundary conditions.

The CFD model developed in the present paper will be the basis for the post-test CFD analysis of the NACIE-UP FPS test section. The subsequent assessment of the methodology and of the model by the direct comparison with experimental data will qualify CFD for wire-wrap bundles cooled by heavy liquid metal.

REFERENCES

1. H.A. Abderrahima, P. Kupschusa, E. Malambua, Ph. Benoita, K. Van Tichelen, B. Ariena, F. Vermeerscha, P. D'hondta, Y. Jongenb, S. Ternierb, D. Vandeplassche, "MYRRHA: A multipurpose accelerator driven system for research & development", *Nuclear Instruments and Methods in Physics Research A*, **vol. 463**, pp. 487-494 (2001).
2. P. Turrone, L. Cinotti et al., "The CIRCE Test Facility", *ANS Winter Meeting*, Reno (2001)
3. I. Di Piazza, P. Gaggini, M. Tarantino, M. Granieri, "The fuel rod bundle design for the NACIE facility", *ENEA SEARCH project, deliverable (D-N°2.1)*, (2012).
4. R. Gajapathy, K. Velusamy, P. Selvaraj, P. Chellapandi, S.C. Chetal, "CFD investigation of helical wire-wrapped 7-pin fuel bundle and the challenges in modelling full scale 217 bundle", *Nuclear Engineering and Design*, **vol. 237 (24)**, pp. 2332–2342 (2007)
5. J. Lafay et al., *ASME paper 75-HT-22* (1975).
6. T.B. Barholet et al., CRBRP-ARD-0108 (January 1977).
7. T.G. Bartholet et al., WARD-D-0161 (October 1976).
8. N. Todreas, Personal communications, *MIT*, to A.A. Bishop (1979).
9. R. Gajapathy, K. Velusamy, P. Selvaraj, P. Chellapandi, S.C. Chetal, "CFD investigation of helical wire-wrapped 7-pin fuel bundle and the challenges in modelling full scale 217 bundle", *Nuclear Engineering and Design*, **vol. 237 (24)**, pp. 2332–2342 (2007)
10. R. Gajapathy, K. Velusamy, P. Selvaraj, P. Chellapandi, S.C. Chetal, "A comparative CFD investigation of helical wire-wrapped 7, 19 and 37 fuel pin bundles and its extendibility to 217 pin bundle", *Nuclear Engineering and Design*, **vol. 239**, pp. 2279–2292 (2009).
11. ANSYS CFX Release 15 User Manual.
12. X. Cheng, N.I. Tak, "CFD analysis of thermal-hydraulic behavior of heavy liquid metals in sub-channels", *Nuclear Engineering and Design*, **vol. 236**, pp.1874-1885 (2006).
13. OECD/NEA, "Handbook on Lead-bismuth Eutectic Alloy and Lead Properties Materials Compatibility Thermal-hydraulics and Technologies", *NEA 6195*, (2007).
14. M.H. Fontana, "Temperature Distribution in the Duct Wall and at the Exit of a 19-Rod Simulated LMFBR Fuel Assembly (FFM-2A)", *ORNL-4852*, Oak Ridge National Laboratory (1973).
15. R. Marinari, "Pre-Test CFD Analysis of the rod bundle experiment in the heavy liquid metal facility NACIE-UP", *Master Thesis*, University of Pisa (2014).
16. K. Rehme, Pressure drop correlations for fuel element spacers. *Nuclear Technology* **vol. 17**, pp. 15–23 (1973).
17. S.K. Cheng, N.E. Todreas, "Hydrodynamic models and correlations for bare and wire-wrapped hexagonal rod bundles - bundle friction factors, sub-channel friction factors and mixing parameters", *Nuclear Engineering and Design*, **vol. 92**, pp. 227–251 (1986).
18. P.A. Ushakov, A.V. Zhukov and M.M. Matyukhin, "Heat transfer to liquid metals in regular arrays of fuel elements", *High Temperature* 15 pp. 868–873; translated from *Teplofizika Vysokikh Temperatur* 15 (5), pp. 1027–1033 (1977).
19. K. Mikityuk, Heat transfer to liquid metal: Review of data and correlations for tube bundles, *Nuclear Engineering and Design*, **vol. 239**, pp. 680–687, (2009).